http://dx.doi.org/10.5012/bkcs.2012.33.2.601

Synthesis and Photoluminescence of Colloidal Solution Containing Layered Rare-earth Hydroxide Nanosheets

Byung-Il Lee, Jung-soo Bae, Eun-su Lee, and Song-Ho Byeon*

Department of Applied Chemistry, College of Applied Science, Kyung Hee University, Gyeonggi 446-701, Korea
**E-mail: shbyun@khu.ac.kr*
Received October 15, 2011, Accepted December 14, 2011

An aspect of organophilic modification for the delamination is described for the layered rare-earth hydroxides in this paper. The interlayer property of $RE_2(OH)_5NO_3 \cdot nH_2O$, where RE=Eu (LEuH) and Tb (LTbH), was modified by the exchange reaction of nitrate ion with oleate anion that is one of the representative dispersion agents in nonpolar solvents. The bilayer arrangement of long oleate anions in the gallery of $RE_2(OH)_5NO_3 \cdot nH_2O$ could effectively weaken the stacking of the hydroxide layers. Highly organophilic environment of the interlayer space promoted the introduction of toluene to delaminate the layered structure into their individual sheets. When irradiated with 365 nm UV, the resulting transparent colloidal solutions of toluene containing LEuH and LTbH nanosheets yielded typical red and green emissions, respectively, which are visible to the naked eye.

Key Words : Colloidal solution, Rare-earths, Photoluminescence, Layered hydroxides, Nanosheets

Introduction

Colloidal solutions containing the inorganic monolayers of ultimate two-dimensional anisotropy can be produced by the delamination of layered compounds. The classical example would refer to the infinite swelling of clay minerals.[1,2] When the layer charge density is high, the colloidal suspension is obtained by an interlayer modification of minerals.[3,4] The clay minerals are delaminated to generate the negatively charged nanosheets which can be considered as macroanions. Several layered compounds such as metal phosphates,[5] transition-metal dichalcogenides,[6] and metal oxides[7,8] were previously delaminated through the similar modification process including the exchange reaction of interlayer ions.

The layered double hydroxides (LDHs), known as anionic clays, can generate the positively charged nanosheets, which are complementary to such negatively charged sheets. However, a high charge density of layers attributed to a high content of anionic species and water molecules causes a strong electrostatic interactions between the layers of LDHs.[9] Consequently, the colloidal solution of LDHs has been frequently obtained after modifying the interlayer region with intercalated organic anions[10-12] or small inorganic anions.[13,14] The delaminated LDH nanosheets were used to fabricate the composite thin films,[7,15] nanocomposites with organic polymers,[16,17] and hollow spheres.[18]

Recently, a series of layered compounds consisting of pure cationic rare-earth hydroxide layers have been reported by several authors[19-23] and briefly reviewed.[24] This class of compounds, called the layered rare-earth hydroxides (LRHs), is represented by the general formula $RE_2(OH)_5X \cdot nH_2O$ where X is the organic or inorganic interlayer anions. LRHs are structurally similar to LDHs and composed of alternating positively charged hydroxocation layers and charge-compensating anion layers. Owing to the capacity to take high payload of guest molecules with high affinity, the family of LRHs is the attractive layered host material for a wide range of active molecules. Furthermore, the magnetic resonance relaxation property of the colloidal solution of layered gadolinium hydroxychloride ($Gd_2(OH)_5Cl \cdot nH_2O$) exhibited the sufficient positive contrast effect for magnetic resonance imaging (MRI).[25] However, while their structural characteristics as a layered compound have been well demonstrated, the colloidal solutions of LRH nanosheets have not yet been well investigated. Although it was reported that LRHs and LRHs containing the alkali-metal salts in the interlayer gallery can produce the formamide and aqueous colloidal suspension, respectively,[26,27] an improvement of the concentration and stability of colloidal solutions is still challenging for the wide field of applications.

In general, the intercalation of long chain organic molecules or surfactants into the layered materials can separate the layers apart from each other, giving a large interlayer spacing. If the solvent molecules are able to solvate the hydrophobic tails of molecules intercalated into the interlayer space, the delamination of layers is then facilitated in such solvents. In our previous study,[28] the hydrophobic sheets of oleate exchanged-gadolinium hydroxide could be rendered hydrophilic by the phospholipids with poly(ethylene glycol) tail groups. The resulting aqueous colloidal suspension of fluorescent gadolinium hydroxide sheets showed a potential as a multimodal probe combining optical and MR imaging. In an attempt to further understand the colloidal solution containing rare-earth hydroxide nanosheets, our effort was made to prepare the transparent colloidal solutions of LRH family in nonpolar solvents. In this paper, we describe the general aspect of organophilic modification of hydroxide layers for delamination and the photolumine-

scence behaviour of the colloidal suspensions in toluene. Because the Eu^{3+} and Tb^{3+} cations are widely applied for the red- and green-emission, respectively, RE=Eu and Tb members of $RE_2(OH)_5NO_3{\cdot}nH_2O$ family were selected.

Experimental

Materials. Any reagent including RE_2O_3 and $RE(NO_3)_3{\cdot}6H_2O$ (RE = Eu and Tb) and sodium oleate was used as purchased without any purification.

Preparation of LEuH and LTbH. Layered europium hydroxynitrate (LEuH) and layered terbium hydroxynitrate (LTbH) were synthesized *via* a hydrothermal reaction.[21] Typically, ~1.5 g of RE_2O_3 (RE = Eu and Tb) was dissolved in 40 mL of 10% HNO_3 solution. After clear solution was formed by uniform stirring, aqueous KOH (10%) solution was dropwise added with vigorous stirring at room temperature until the pH of solution was adjusted to 6.5-6.9 at 30 °C. The resulting mixtures for LEuH and LTbH were put into a Teflon-lined stainless steel autoclave with a capacity of 100 mL. The autoclave was sealed and maintained at 130-160 °C for 12-16 hr. The solution was continuously stirred during the solvothermal treatment. The reaction temperature was then lowered to 60 °C for aging for 12 hr. After the reaction was completed, the solid product was collected by filtration, washed with distilled water, and dried at 40 °C for a day.

Exchange Reaction between NO_3 and Oleate Anion. Intercalation of oleate anions was achieved using the ion-exchange method. In a typical synthesis of LEuH-OA and LTbH-OA, 0.25 g of LRH powder was dispersed into an aqueous anionic solution containing 3-fold molar excess of sodium oleate. The ion-exchange reaction between NO_3 and oleate ($C_{17}H_{33}COO^-$) anions was carried out at room temperature for 24 hr in air while stirring. Resulting precipitates were recovered by filtration, washed with water, and dried at 40 °C for a day.

Preparation of Colloidal Solutions of LEuH and LTbH. Delamination was accomplished by adding LEuH-OA and LTbH-OA (0.2-1.0 g) in 50.0 mL of toluene. To facilitate the delamination, the dispersion was ultrasonically treated in successive intervals of 10 min. A translucent colloidal solution was yielded after repeated ultrasonic treatments of the mixtures within 1 hr at room temperature, suggesting the occurrence of delamination. To remove possible unexfoliated particles, the resulting suspensions were further treated by centrifugation at 2000 rpm for 5 min before analyses.

Characterization. The chemical compositions of LRHs and LRH-OAs were confirmed by inductively coupled plasma (ICP; Thermo Elemental Thermo ICAP 6000), thermogravimetry (TG; Seiko Instruments TG/DTA320 SSC/5200 S11), and elemental analysis (EA; CE Instruments Flash EA1112). The powder X-ray diffraction patterns were recorded on a rotating anode installed diffractometer (MacScience Model M18XHF). The Cu Kα radiation used was monochromated by a curved-crystal graphite. Field emission scanning electron microscopy (FE-SEM) was carried out with a Carl Zeiss LEO SUPRA 55 electron microscope operating at 30 kV. Specimens for electron microscope were coated with Pt-Rh for 180 s under vacuum. Transmission electron microscopy (TEM) and selected area electron diffraction (SAED) observations were made with a JEOL JEM-2100F electron microscope operating at 300 kV. Atomic force microscopy (AFM) was carried out by using Pucostation STD. To deposit the nanosheets on the substrate, the Si wafer was cleaned successively with methanol/HCl solution and concentrated H_2SO_4, rinsed with deionized water, and dried by high purity N_2 gas. The surface of Si wafer was then hydrophobically primed with a microwave treated CH_4 + Ar mixed gas for 5 min. The substrate was then dipped in a colloidal suspension (0.1 g L^{-1}) of LRH nanosheets for 30 min, washed with toluene several times, and dried with a nitrogen gas flow. The photoluminescence spectra were measured at room temperature using FP-6600 spectrophotometer (JASCO) with a Xenon flash lamp. The emission spectra were recorded at the excitation wavelength with a maximum intensity.

Results and Discussion

Synthesis and Structure of Pristine LEuH and LTbH. General structure of well known layered double hydroxides (LDHs) is compared with that of LRHs in Figure 1. The (transition) metal cations are coordinated mainly by six intralayer OH groups in LDHs. Interlayer water molecules are often coordinated to the metal cations in the layer,

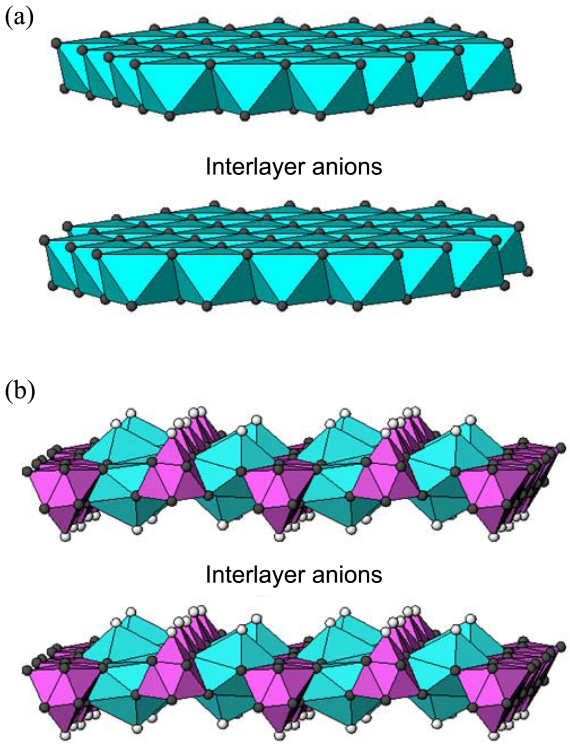

Figure 1. Schematic comparison of the structures for (a) layered double hydroxide (LDH) and (b) layered rare-earth hydroxide (LRH). Gray and white spheres represent the oxygen atoms from intralayer OH groups and interlayer H_2O, respectively.

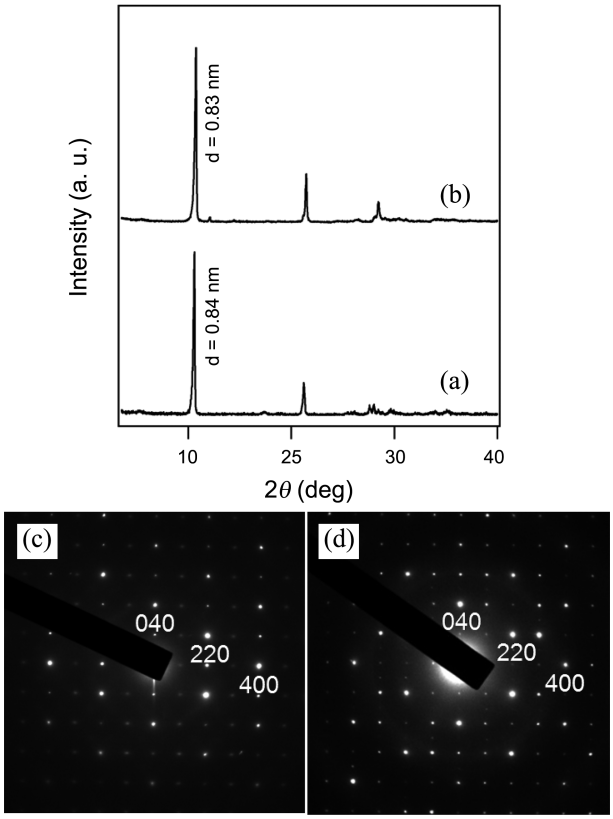

Figure 2. (a, b) Powder X-ray diffraction patterns and (c, d) SAED patterns of LEuH and LTbH, respectively.

providing seven-coordinated sites. Although the rare-earth elements doped LDHs have been reported,[29] their sizes are too large to be stabilized in such coordination polyhedra. Instead, the trivalent rare-earth cations in LRHs occupy the eight-coordinated and the nine-coordinated sites formed by the intralayer OH groups and the interlayer water molecules (Figure 1(b)).[19,22,23] Nevertheless, the structures of LDHs and LRHs are quite similar to each other. The OH groups in the layer of both structures are shared by three polyhedral cations and their hydrogen atoms are directed to the interlayer space.

Figures 2(a) and (b) show the powder X-ray diffraction (XRD) patterns of layered europium hydroxynitrate (LEuH) and layered terbium hydroxynitrate (LTbH). The strong (00*l*) reflections, which are characteristic of a layered phase, are ascribed to the interlayer separation of ~0.83 nm. Because of very weak intensity and insufficient number of non-(00*l*) reflections observed, the arrangement mode within the *ab* plane was measured by the selected area electron diffraction (SAED). As observed in Figures 2(c) and (d), the rectangularly arranged spots are also typical patterns indicating an order within the *ab* plane of LRHs. The determined lattice parameters are a = 0.75 and 0.74 nm and b = 1.32 and 1.31 nm for LEuH and LTbH, respectively. The composition of these compounds was confirmed to be $Eu_2(OH)_5NO_3{\cdot}H_2O$ and $Tb_2(OH)_5NO_3{\cdot}H_2O$ ($n \sim 1.0$) by inductively coupled plasma (ICP), thermogravimetry (TG), and elemental analysis (EA). All the results were in agreement with those of previous reports.[20-23]

Aspect of Interlayer Modification. The anion-exchange reaction was carried out to modify the interlayer characteristics of LRHs so that they undergo an efficient delamination to produce a stable colloid in an appropriate solvent. It is known that the classical LDHs containing surfactants have been successfully delaminated in various solvents.[10-12,30] Therefore, after comparative study for modifying LRHs with several anionic surfactants, the oleate ($C_{17}H_{33}COO^-$) that is one of the representative dispersion agents in nonpolar solvents was selected to achieve highly efficient delamination.[28] The replacement of NO_3 by the oleate anions was confirmed by the disappearance of characteristic reflections of the host LRH lattices in XRD patterns. The chemical compositions of oleate-exchanged derivatives (LEuH-OA and LTbH-OA), determined by ICP and EA are summarized in Table 1. Similarly to that of the host materials, the amount of interlayer water was variable depending on the synthetic conditions. The absence of nitrogen in the oleate-exchanged

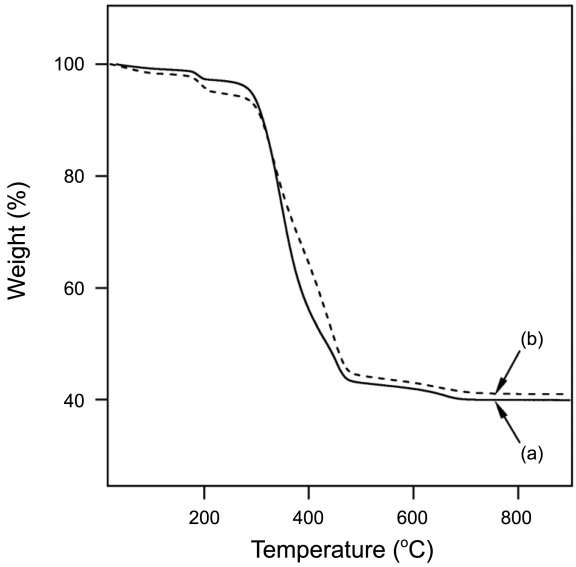

Figure 3. Thermogravimetric (TG) analysis curves of oleate exchanged derevatives; (a) $Eu_2(OH)_5(oleate){\cdot}nH_2O$ and (b) $Tb_2(OH)_5(oleate){\cdot}nH_2O$.

Table 1. Elemental analysis data for the oleate-exchanged products of LEuH and LTbH

Compound	Elemental analysis (%)		Basal spacing (nm)
	Observed	Calculated	
$Eu_2(OH)_5(C_{17}H_{33}CO_2)(C_{17}H_{33}CO_2H)_{0.65}{\cdot}1.5H_2O$	C(41.05), H(7.40)	C(40.49), H(7.22)	4.63
$Tb_2(OH)_5(C_{17}H_{33}CO_2)(C_{17}H_{33}CO_2H)_{0.60}{\cdot}2H_2O$	C(41.39), H(7.87)	C(38.87), H(7.07)	4.59

Table 2. Comparison of the observed and calculated values for water evolution and total ignition loss of the oleate-exchanged products of LEuH and LTbH

Chemical formula	H_2O evolution (%)		Total weight loss (%)	
	Observed	Calculated	Observed	Calculated
$Eu_2(OH)_5(C_{17}H_{33}CO_2)(C_{17}H_{33}CO_2H)_{0.65}\cdot 1.5H_2O$	2.94	3.07	60.08	60.05
$Tb_2(OH)_5(C_{17}H_{33}CO_2)(C_{17}H_{33}CO_2H)_{0.60}\cdot 2H_2O$	4.34	4.05	59.01	58.89

products supported a completion of exchange reaction. Figure 3 shows the TG curves of LEuH and LTbH exchanged with oleate anions. The weight loss below 200 °C corresponds to the amount of cointercalated water. If we consider that the heat treatment of layered hydroxides above 800 °C yields the corresponding oxides, the observed total weight losses are close to those calculated from the proposed chemical formula as compared in Table 2.

It is noted that the elemental analysis data for both LEuH-OA and LTbH-OA exhibited a higher amount of carbon than was anticipated from the amount of oleate needed to balance the charge of the layers. No change in the amount of oleate was observed even after several repeated washings with water or nonpolar solvents, implying a significant interaction between the excess oleate units and the hydroxide matrix. When we extensively washed LRH-OAs with organic solvent such as toluene and chloroform, the delamination process was initiated. Because ICP analysis revealed no sodium content in LRH-OAs, a possibility of incorporation as oleate sodium salt could be ignored. A strong lateral dispersion interaction between long chain alkyl ions often induces an inclusion exceeding the exchange capacity.[21,31,32] It is accordingly postulated that the neutral oleic acid might be incorporated in the interlayer space of LRHs with the maintenance of charge neutrality. An intercalation of excess guest molecules has been also observed in the LDH-phosphonates, where a rapid proton exchange was supposed between the neutral phosphonic acid and phosphonate or between phosphonate units and the interlayer water molecules.[33]

As can be seen in Figure 4, XRD patterns of LRH-OAs display a series of intense basal (00*l*) reflections in the region of low diffraction angle, indicating the incorporation of long oleate anions into the interlayer galleries of LRHs. The interlayer spacings of LEuH-OA and LTbH-OA calculated from the systematic indexation of (00*l*) reflections were 4.63 and 4.59 nm, respectively (Table 1). The arrangement mode of organic hydrocarbon chains in the interlayer space is often different depending on the nature of hosts and functional groups. It has been proposed that the hydrocarbon chains stand vertically or tilt at an angle with respect to the host layer so as to form interdigitating monolayer, normal bilayer, or partly interpenetrating bilayers.[34-36] Considering the expected length of oleate chain (~2.2 nm), the expansion of interlayer spacing from ~0.84 to ~4.6 nm after intercalation of oleate anions is too large to be accounted for by a monolayer arrangement of anions between the layers. According to the packing mode of oleate (*cis*-isomer) and elaidate (*trans*-isomer) in the interlayer of LDHs,[37] the interlayer separations are predicted to be ~3.6 nm and ~4.8 nm for a

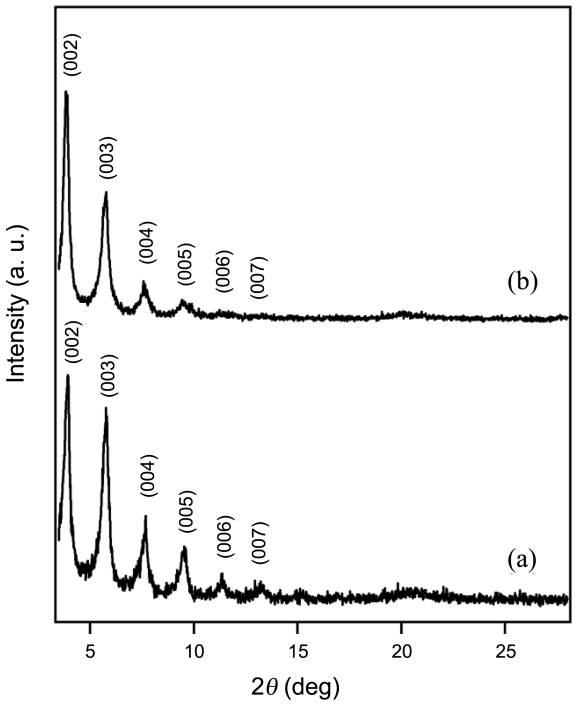

Figure 4. Powder X-ray diffraction patterns of (a) LEuH-OA and (b) LTbH-OA.

partially interdigitated mode and a bilayer packing mode, respectively. Therefore, a bilayer model could be adopted for LRH-OA in the present work. The incorporation of excess neutral oleic acid might be responsible for the bilayer arrangement. An effective lateral hydrophobic interaction with excessively intercalated oleic acid molecules would keep the oleate anions from interpenetrating each other. The formation of bilayer has also been observed with different organic carboxylate exchanged-LRHs.[21] Transmission electron microscopy (TEM) images of LEuH-OA and LEuH-OA are shown in Figure 5. The observed fringes are associated with the regular crystalline lattices. The distance between fringes is close to 4.7 nm, which is comparable with the interlayer spacings determined from XRD patterns of LEuH-OA and LEuH-OA (Figure 4).

Colloidal Solutions. An appropriate combination of interlayer ion and solvent has been used to promote the delamination of two-dimensionally ordered structures. It was found that the nonpolar solvents such as toluene and chloroform can effectively solvate the hydrophobic layers of LRHs modified by oleate anions. The stable colloidal solution was then obtained by delaminating LEuH-OA and LTbH-OA in toluene. The exfoliation process was significantly accele-

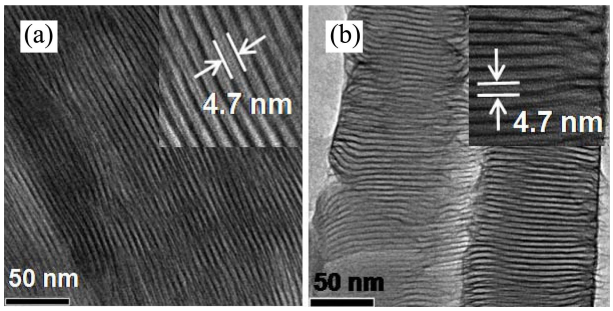

Figure 5. TEM images of (a) LEuH-OA and (b) LTbH-OA.

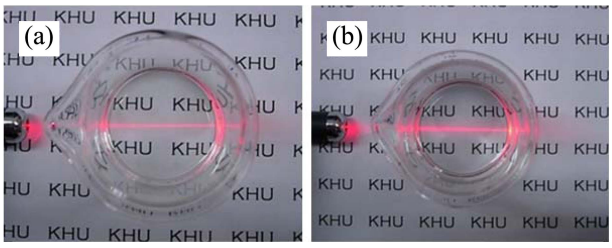

Figure 6. Photographs of colloidal suspension containing delaminated nanosheets of (a) LEuH and (b) LTbH in toluene (1.0 gL^{-1}). The light beam was irradiated from the side to demonstrate the Tyndall effect.

rated by ultrasonication. The kind of interlayer anions have great effects on the delamination behaviors of LRHs. For instance, the dodecylsulfate (DS) anion would be one of the most frequently used surfactants to delaminate the classical LDHs.[10-12,38] It is of interest that, when they were intercalated into the interlayer of LRHs, the dodecylsulfate anions are arranged in a tilted monolayer mode. Elemental analysis of resulting LRH-DS suggested that no excess dodecylsulfate group was intercalated in the interlayer space. The delamination of LRH-DS was much less efficient in comparison with LRH-OA at room temperature.

As shown in Figure 6, the laser illumination to the suspensions (1.0 gL^{-1}) of LEuH-OA and LTbH-OA in toluene demonstrates the clear Tyndall light scattering, supporting the presence of abundant delaminated nanosheets dispersed in toluene. The colloidal suspensions of LRH-OAs were stable and no aggregated sediment was observed for more than a month. Figure 7 shows typical SAED patterns of LEuH and LTbH nanosheets which were taken from a randomly chosen particles in the colloidal solutions. The clear spots indicate their crystalline nature. The rectangular arrangements of spots are consistent with those of pristine LRHs (Figure 2).[20,21] The estimated lattice parameters of a = 0.75 and 0.73 nm and b = 1.32 and 1.30 nm are also comparable with the in-plane structural parameters of LEuH and LTbH host crystals, respectively. This agreement unambiguously indicates that the intralayer structure of LRHs remains unchanged during the anion-exchange reactions followed by the delamination. The size and thickness of the delaminated nanosheets were examined by AFM. In Figure 8, the lateral dimensions of thin sheetlike objects detected by AFM observations are in the range of 50-200 nm. The height profiles along the

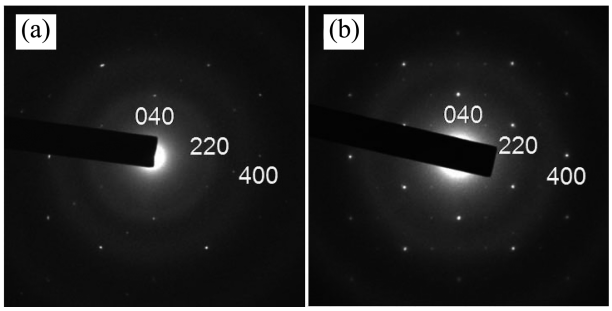

Figure 7. SAED patterns of delaminated (a) LEuH and (b) LTbH nanosheets.

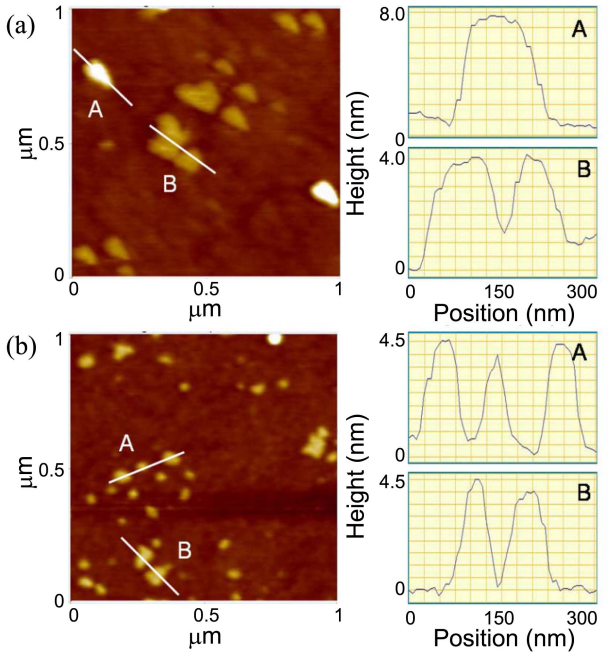

Figure 8. AFM images and height profiles of (a) LEuH and (b) LTbH nanosheets deposited on Si wafer.

white lines in the images reveal two distinct thicknesses of ~4 nm and ~8 nm. By considering the ~4.6 nm basal spacing of LEuH-OA and LTbH-OA, such thicknesses suggest that the majority of nanosheets delaminated in the suspension consists of one or two monolayers carrying oleate anions at the external surface.

Photoluminescence Spectra of Colloidal Solutions. When irradiated with 365 nm UV, the transparent colloidal solutions of toluene containing LEuH and LTbH nanosheets yielded a red and green emission, respectively, which are visible to the naked eye as shown in Figure 9 (insets). Such characteristic colors of the UV irradiated suspensions support again the presence of europium and terbium hydroxide nanosheets dispersed in toluene. The excitation spectrum of LEuH colloidal solution consisted of a series of bands with a maximum at about 397 nm, which were attributed to the f-f transitions in the Eu^{3+} ($4f^6$), $^7F_0 \rightarrow {}^5D_4$ (365 nm), $^7F_0 \rightarrow {}^5L_7$ (383 nm), and $^7F_0 \rightarrow {}^5L_6$ (397 nm). Figure 9(a) displays the photoluminescence (PL) emission spectra of LEuH powder and colloidal solution, which were excited at 397 nm. The

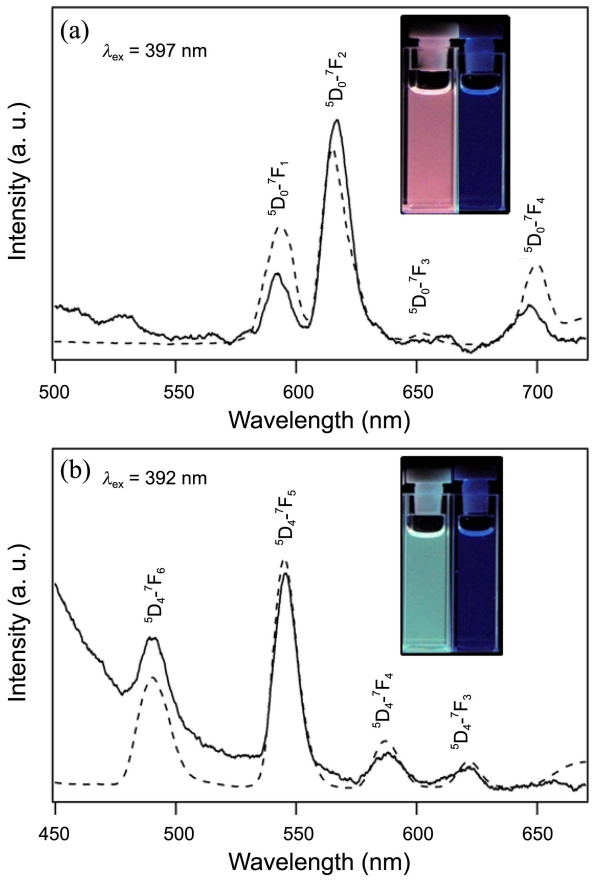

Figure 9. Emission spectra (solid lines) of colloidal solution containing (a) LEuH and (b) LTbH nanosheets. The emission spectra of corresponding powders are represented by dotted lines. Insets: photographs of toluene (right) and the transparent suspensions (left) emitting characteristic red and green colors visible to the naked eye under UV (365 nm) irradiation.

observed emission bands are assigned to $^5D_0 \rightarrow {}^7F_1$, $^5D_0 \rightarrow {}^7F_2$, $^5D_0 \rightarrow {}^7F_3$, and $^5D_0 \rightarrow {}^7F_1$ transitions.[39] In particular, the sharp and intense band centered at around 615 nm and ascribed to the $^5D_0 \rightarrow {}^7F_2$ transition causes a red color of colloidal solution containing LEuH nanosheets. The intensity of magnetic dipole transition ($^5D_0 \rightarrow {}^7F_1$) is independent on the site symmetry of Eu^{3+} ions while the forced electric dipole transition ($^5D_0 \rightarrow {}^7F_2$) is sensitive to the symmetry of site occupied with Eu^{3+} ion in the host.[40,41] Therefore, the intensity ratio between two emissions ($^5D_0 \rightarrow {}^7F_2$)/($^5D_0 \rightarrow {}^7F_1$), called the asymmetric ratio,[42] can be a measure of distortion from the inversion symmetry around Eu^{3+} ion. The eight-coordinated and the nine-coordinated sites for Eu^{3+} cations are formed by both the intralayer OH groups and the interlayer water molecules in the pristine LEuH.[19,22,23] A significant difference in the asymmetric ratio (I_{615}/I_{593}) between the powder (dotted line) and the colloidal solution (solid line) in Figure 9(a) would indicate that the distortion from the inversion symmetry of the local environment around Eu^{3+} is enhanced by the release of weakly coordinated water molecules after delamination.

In the excitation spectrum of LTbH colloidal solution monitored at 545 nm, the highest intensity band assigned to the $^5D_3 \rightarrow {}^7F_6$ transition of Tb^{3+} ($4f^8$) was observed at about 372 nm. Thus the colloidal solution of LTbH could be well excited at 372 nm. The PL emission spectrum of colloidal solution (solid line) is compared with that (dotted line) of pristine LTbH powder in Figure 9(b). Trivalent terbium (Tb^{3+}) has been recognized as a blue-green luminescent center as a result of $^5D_4 \rightarrow {}^7F_J$ (J = 6, 5, 4, 3) transitions.[39] The bands assigned to the $^5D_4 \rightarrow {}^7F_6$ (490 nm) and $^5D_4 \rightarrow {}^7F_5$ (545 nm) transitions correspond to the blue and green emission, respectively. It is accordingly evident that the most intense emission centered at 545 nm is responsible for a green color of UV irradiated colloidal solution containing LTbH nanosheets.

Conclusion

We demonstrated that the oleate (surfactant) and toluene (solvent) is an effective combination for producing the colloidal solution of layered compounds that consist of purely cationic europium and terbium hydroxide layers. This approach can be exploited as a general method employable for the complete series of rare-earth cations. The development of colloidal suspension containing the rare-earth hydroxide nanosheets could broaden further the application field of rare-earth materials as it accesses interesting new catalysts, polymer/rare-earth nanocomposites, and bioactive nanocomposite materials. Furthermore, the rare-earth cations applicable as a luminescent center exhibit their characteristic photoluminescence after delamination in an appropriate solvent, which are visible to the naked eye.

Acknowledgments. This work was supported by Mid-career Researcher Program through National Research Foundation (NRF) grant funded by the Ministry of Education, Science and Technology (MEST) (No. 2011-0014763).

References

1. Jimenez de Haro, M. C.; Perez-Rodriguez, J. L.; Poyato, J.; Perez-Maqueda, L. A.; Ramirez-Valle, V.; Justo, A.; Lerf, A.; Wagner, F. E. *Appl. Clay Sci.* **2005**, *30*, 11.
2. Saunders, J. M.; Goodwin, J. W.; Richardson, R. M.; Vincent, B. *J. Phys. Chem. B* **1999**, *103*, 9211.
3. Thostenson, E. T.; Li, C.; Chou, T.-W. *Composites Sci. Technol.* **2005**, *65*, 491.
4. Tenne, R. *Angew. Chem. Int. Ed.* **2003**, *4*, 5124.
5. Alberti, G.; Cavalaglio, S.; Dionigi, C.; Marmottini, F. *Langmuir* **2000**, *16*, 7663.
6. Divigalpitiya, W. M. R.; Frindt, R. F.; Morrison, S. R. *Science* **1989**, *246*, 369.
7. Osada, M.; Sasaki, T. *J. Mater. Chem.* **2009**, *19*, 2503.
8. Shukoor, M. I.; Therese, H. A.; Gorgishvili, L.; Glasser, G.; Kolb, U.; Tremel, W. *Chem. Mater.* **2006**, *18*, 2144.
9. Albiston, L.; Franklin, K. R.; Lee, E.; Smeulders, J. B. A. F. *J. Mater. Chem.* **1996**, *6*, 871.
10. O' Leary, S.; O'Hare, D.; Seeley, G. *Chem. Commun.* **2002**, 1506.
11. Leroux, F.; Adachi-Pagano, M.; Intissar, M.; Chauviere, S.; Forano, C.; Besse, J. P. *J. Mater. Chem.* **2001**, *11*, 105.
12. Adachi-Pagano, M.; Forano, C.; Besse, J. P. *Chem. Commun.* **2000**, 91.
13. Liu, Z.; Ma, R.; Osada, M.; Iyi, N.; Ebina, Y.; Takada, K.; Sasaki,

T. *J. Am. Chem. Soc.* **2006**, *128*, 4872.
14. Wu, Q. L.; Olafsen, A.; Vistad, O. B.; Roots, J.; Norby, P. *J. Mater. Chem.* **2005**, *15*, 4695.
15. Okamoto, K.; Sasaki, T.; Fujita, T.; Iyi, N. *J. Mater. Chem.* **2006**, *16*, 1608.
16. Qiu, L.; Qu, B. *J. Colloid Interface Sci.* **2006**, *301*, 347.
17. Moujahid, E. M.; Besse, J.-P.; Leroux, F. *J. Mater. Chem.* **2002**, *12*, 3324.
18. Li, L.; Ma, R.; Iyi, N.; Ebina, Y.; Takada, K.; Sasaki, T. *Chem. Commun.* **2006**, 3125.
19. Gandara, F.; Perles, J.; Snejko, N.; Iglesias, M.; Gomez-Lor, B.; Gutierrez-Puebla, E.; Monge, M. A. *Angew. Chem. Int. Ed.* **2006**, *45*, 7998.
20. McIntyre, L. J.; Jackson, L. K.; Fogg, A. M. *Chem. Mater.* **2008**, *20*, 335.
21. Lee, K.-H.; Byeon, S.-H. *Eur. J. Inorg. Chem.* **2009**, 929.
22. Poudret, L.; Prior, T. J.; McIntyre, L. J.; Fogg, A. M. *Chem. Mater.* **2008**, *20*, 7447.
23. Geng, F.; Matsushita, Y.; Ma, R.; Xin, H.; Tanaka, M.; Izumi, F.; Iyi, N.; Sasaki, T. *J. Am. Chem. Soc.* **2008**, *130*, 16344.
24. Geng, F.; Ma, R.; Sasaki, T. *Acc. Chem. Res.* **2010**, *43*, 1177.
25. Lee, B.-I.; Lee, K. S.; Lee, J. H.; Lee, I. S.; Byeon, S.-H. *Dalton Trans.* **2009**, 2490.
26. Lee, K.-H.; Byeon, S.-H. *Eur. J. Inorg. Chem.* **2009**, 4727.
27. Lee, K.-H.; Lee, B.-I.; You, J.-H.; Byeon, S.-H. *Chem. Commun.* **2010**, *46*, 1461.
28. Yoon, Y.-S.; Lee, B.-I.; Lee, K. S.; Im, G. H.; Byeon, S.-H.; Lee, J. H.; Lee, I. S. *Adv. Funct. Mater.* **2009**, *19*, 3375.
29. Birjega, R.; Pavel, O. D.; Costentin, G.; Che, M.; Angelescu, E. *Appl. Catal. A* **2005**, *288*, 185.
30. Guo, Y.; Zhang, H.; Zhao, L.; Li, G. D.; Chen, J. S.; Xu, L. *J. Solid State Chem.* **2005**, *178*, 1830.
31. Trujillano, R.; Holgado, M. J.; Pigazo, F.; Rives, V. *Physica B* **2006**, *373*, 267.
32. Kloprogge, J. T.; Frost, R. L. *J. Solid State Chem.* **1999**, *146*, 506.
33. Williams, G. R.; O'Hare, D. *Solid State Sciences* **2006**, *8*, 971.
34. Li, B.; He, J. *J. Phys. Chem. C* **2008**, *112*, 10909.
35. Xu, Z. P.; Braterman, P. S. *J. Mater. Chem.* **2003**, *13*, 268.
36. Carlino, S. *Solid State Ionics* **1997**, *98*, 73.
37. Xu, Z. P.; Braterman, P. S.; Yu, K.; Xu, H.; Wang, Y.; Brinker, C. J. *Chem. Mater.* **2004**, *16*, 2750.
38. Ida, S.; Shiga, D.; Koinuma, M.; Matsumoto, Y. *J. Am. Chem. Soc.* **2008**, *130*, 14038.
39. Blasse, G.; Grabmaier, B. C. *Luminescence Materials*; Springer: Berlin, Heidelberg, 1994.
40. Judd, B. R. *Phys. Rev.* **1962**, *127*, 750.
41. Ofelt, G. S. *J. Chem. Phys.* **1962**, *37*, 511.
42. Vicentini, G.; Zinner, L. B.; Zukerman-Schpector, J.; Zinner, K. *Coord. Chem. Rev.* **2000**, *196*, 353.